Synthesis of polyethylene-based covalent adaptable networks including 1,2,3-triazolium or imine dynamic cross-links by reactive processing

Benedetta Rigatelli, Damien Montarnal, Eric Drockenmuller

Synthesis of polyethylene-based covalent adaptable networks including 1,2,3-triazolium or imine dynamic cross-links by reactive processing

Benedetta Rigatelli[a,b], Damien Montarnal[b], and Eric Drockenmuller*[a]*

[a]Université Claude Bernard Lyon 1, CNRS, Ingénierie des Matériaux Polymères, UMR 5223, Villeurbanne, F-69100, France.

[b]Université Claude Bernard Lyon 1, CPE Lyon, CNRS, Catalyse, Polymérisation, Procédés et Matériaux, UMR 5128, Villeurbanne, F-69100, France.

* Corresponding authors.
E-mail address: damien.montarnal@univ-lyon1.fr (D. Montarnal),
eric.drockenmuller@univ-lyon1.fr (E. Drockenmuller)

KEYWORDS:

Polyethylene

Covalent adaptable network

Cross-linking

Imine

1,2,3-triazolium

HIGHLIGHTS

- Imine- and 1,2,3-triazolium-containing diamine cross-linkers are synthesized
- Polyethylene-based covalent adaptable networks are prepared by reactive processing
- Amine groups react with pendent anhydrides from a commercial polyethylene
- Orthogonality between grafting and exchange reactions is discussed

TOC ABSTRACT

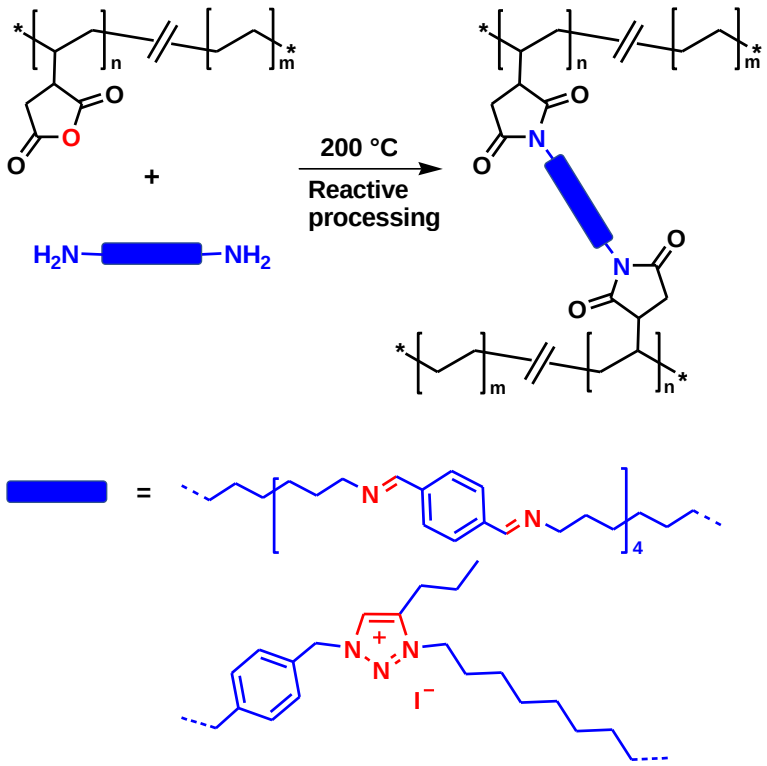

ABSTRACT.

Polyethylene-based covalent adaptable networks (PE CANs) are obtained by reactive extrusion in a micro-compounder of a commercial maleic anhydride-grafted polyethylene (PE-*g*-MA) with two tailor-made α,ω-diamine cross-linkers carrying either imine or 1,2,3-triazolium groups as dissociative covalent dynamic bonds. Depending on the chemical nature of the exchangeable bonds, drastically different properties are demonstrated by FTIR, swelling/extractible, reactive dissolution and rheological experiments. The imine-containing PE CAN yields a high gel fraction but rheology and reactive dissolution experiments demonstrate the lack of dynamicity due to side-reactions promoting the formation of non-dynamic covalent cross-links. Such undesirable reaction occurs already during the processing stage from the premature cleavage of the imine bonds into amines, and further formation of permanent imide cross-links by reaction with pendent maleic anhydrides. Conversely, the 1,2,3-triazolium-containing PE CAN presents a lower gel fraction but exhibits viscoelastic properties typical of dissociative CANs. While this material is easily reprocessable by compression molding, the evolution of the rheological properties at high temperatures (160 to 200 °C) points toward the occurrence of side reactions slowing down the relaxation dynamics which we attribute to the chemical rearrangement of the 1,2,3-triazolium cross-links. These two examples illustrate the difficulty of using *amine*-functionalized dynamic cross-links in the synthesis of PE CANs by reactive extrusion using PE-*g*-MA.

1 Introduction

Covalent adaptable networks (CANs) are gaining increasing impetus due to their malleability that enables multiple reprocessing cycles through compression moulding while presenting solvent resistance and high performance at service temperature typical of thermosets [1–3]. This behaviour results from the presence of exchangeable covalent cross-links that impart dynamicity upon thermal or photochemical activation [4,5]. CANs are divided into two sub-classes according to the mechanism of the covalent exchange reactions, i.e. involving either an associative (also coined as vitrimers) or a dissociative pathway that particularly affects the temperature dependence of the cross-link density [6,7]. A plethora of covalent exchange reactions has been developed during the last decade [8–10] and exploited in a number of CANs, either densely cross-linked thermosets from multifunctional monomers or lightly cross-linked networks from multifunctional oligomers or polymers. In the latter type of CANs, melt reactive processing is the method of choice to graft on the polymer either directly a difunctional cross-linker bearing an internal dynamic bond, or a monofunctional precursor that can later on form a dynamic cross-link. The effective relaxation time of the CAN obtained depends however strongly on the molar mass of the parent polymer because of an interplay between chain dynamics and cross-link exchanges [11], [12]. This strategy has been in particular applied with some success to polyolefins in order to tackle industrially-relevant materials [13]. Leibler, Nicolaÿ and coworkers pioneered the development of polyethylene CANs (PE CANs) by radical grafting of maleimide-functionalized dioxaborolanes onto HDPE using melt reactive processing. The subsequent introduction of bis-dioxaborolanes cross-linkers promotes the formation of dynamic cross-links through dioxaborolane exchanges [14]. Malleability coupled with the persistence of a cross-linked structure above the melting temperature of PE affords a dimensional stability beneficial in a number of applications such as fire retardancy or phase change materials [15], and also applicable to amorphous polyolefin elastomers [16]. Alternatively to the two-step cross-linking process involving grafting of mono dioxaborolanes and further exchange with a difunctional cross-linker, bis-dioxaborolane-containing bis-maleimides [17] or bis-nitroxides [18] were directly grafted onto HDPE, although the resulting materials displayed very high melt viscosities and had to resort to processing aids that decreased the cross-link density in order to lead to proper processing. Direct grafting of dynamic cross-linkers on polyolefins has also been demonstrated using bis methacrylates incorporating an internal dialkylamino disulfide group (BiTEMPS) [19], [20]. Cautious adjunction of peroxide initiator is required to ensure proper grafting, but should be limited to avoid the formation of

non-dynamic permanent cross-links. BiTEMPS groups are very weakly dissociative, with a dissociated fraction well under 10^{-5} at 130 °C [21], and also demonstrate a remarkable thermal stability.

Further extension of PE CANs to various dynamic exchanges could be achieved in a two-steps process : first, maleic anhydride (MA) is grafted, then further functionalization with bisphenol A diglycidyl ether [22], 1,4-butanediol [23], or pentaerythritol tetrakis(3-mercaptopropionate) [24] allows to incorporate β-hydroxyesters, esters or thioesters dynamic bonds. The difficulty to control the content and homogeneity of the radical grafting of polyolefins using MA or maleimides under melt processing rather favours the use of commercially available functional polyolefins with well-controlled functionality due to extensive and efficient quality control at industrial scale. For instance, LLDPE-*g*-MA and HDPE-*g*-MA were reacted in the melt with 4-4'-dithioaniline to yield PE CANs relying on disulfide metathesis covalent exchanges [25], [26]. HDPE-*g*-glycidyl methacrylate were reacted in presence of TBD catalyst with α,ω-dihydroxy poly(tetrahydrofuran) or poly(ε-caprolactone) to afford PE CANs involving the transesterification of β-hydroxyl esters [27]. Other studies on PE CANs also involved the use of polyolefin copolymers comprising a high content of pendent functionalities (i.e. 2.5 to 12 mol%) with significantly decreased crystallinity or even amorphous characteristics. The reactive processing of poly(ethylene-*co*-[2-(methacryloyloxy)ethyl acetoacetate]) with *m*-xylylenediamine afforded PE CANs relying on the trans-amination of vinylogous urethane cross-links [28]. The reactive processing of poly(ethylene-*co*-2-(hydroxyethyl methacrylate)) with *N*,*N*'-bis[3-(trimethoxysilyl)propyl]ethylenediamine afforded PE CANs based on silyl ether covalent exchanges [29]. Diels-Alder reaction between a maleimide-functionalized dioxaborolane and an anthracene-functionalized poly(ethylene-*co*-tetradecene) and further introduction of a bis-dioxaborolane afforded amorphous elastomers involving dioxaborolane metathesis covalent exchanges [30]. The reactive processing of glycidyl-grafted ethylene-octene elastomers with 1,2,4-benzenetricarboxylic acid afforded PE CANs based on transesterification covalent exchanges [31]. Finally, the reactive processing between an aldehyde-functionalized ethylene/propylene copolymer rubber (EPR) and tris-(2-aminoethyl) amine afforded EPR CANs involving imine exchangeable bonds [32].

In the current study, we illustrate some of the difficulties that can arise when grafting dynamic cross-linkers with fast exchange dynamics on a commercially available maleic anhydride grafted polyethylene. Two distinct dissociative exchange reactions. Imines (also known as Schiff bases) have been widely implemented in the field of CANs [33]–[37]. They can undergo

several exchange mechanisms depending on the temperature, the presence of catalyst and surrounding functionalities [38]. In presence of water and optionally an acid catalyst, the covalent exchange mechanism is dissociative and imines reversibly hydrolyse into amine and aldehyde groups [39]. Even in absence of water or catalysts, transimination reactions with minute amounts of amines have also found to be quite efficient even at very low temperatures. [40] In complete absence of catalyst or additional protic functionalities, true imine metathesis has also been claimed but difficult to prove as minute amounts of amines are most of the time present. Therefore, unambiguous distinction between these three reactions occurring within CANs remains challenging and coexistence of more than one exchange mechanism is probable in most systems. CANs including imine covalent exchanges have however gained a lot of attention due to their easy accessibility, mainly from primary amine- and aldehyde-functionalized precursors, their fast exchange dynamics (typically between 1 and 100 s at 150 °C) that are highly dependent on the chemical environment and the presence of catalysts. On the other hand, trans-*N*-alkylation of 1,2,3-triazolium groups has been recently implemented in the field of CANs [41]–[44]. The dissociative covalent exchange mechanism typically involves a de-*N*-alkylation reaction. The covalent exchange kinetics can be widely tuned by the chemical structures of the *N*-1 and *N*-3 substituents of the 1,2,3-triazolium cross-links as well as the counter-anion nucleophilicity [45]. In particular, poly(1,2,3-triazolium)-based CANs combining aliphatic and benzylic *N*-substituents are able to combine fast stress relaxation (down to ca. 50 s at 160 °C) and nearly constant cross-link density in a wide temperature range typical of associative CANs.

Herein, PE CANs were prepared by reactive processing of a commercial HDPE-*g*-MA using a dual screw laboratory compounder in the presence of diamine cross-linkers incorporating imine and 1,2,3-triazolium groups. Their characterization by FTIR spectroscopy, thermogravimetric analysis, swelling/extractible and rheology measurements enabled to relate the temperature dependence of the viscoelastic properties to the involved chemical reactions highlighting the importance of the orthogonality between the cross-linker grafting and covalent exchange reactions.

2 Experimental section

2.1 Materials

Terephthalaldehyde (TA, 99%), hexamethylene diamine (HMDA, 98%), *p*-toluenesulfonic acid (*p*-TSA, 98%), dodecyl amine (DA, 99%) sodium azide (NaN_3, 99%), diisopropylethylamine

(DIPEA, 99%), 1-pentyne (99%), copper(I) iodide-triethylphosphite (CuI.P(OEt)$_3$, 97%), sodium iodide (NaI, 98%), α,α′-dichloro-*p*-xylene (98%), 8-chloro-octan-1-ol (98%), triethylamine (NEt$_3$, 99%), 4-toluenesulfonyl chloride (98%) and triphenylphospine (PPh$_3$, 99%) were purchased from Merck and used as received. 1-Azido-8-iodooctane [46], and 1,4-bis(azidomethyl)benzene [47], were synthesized according to already reported procedures. PE-*g*-MA (Orevac 18507, SK Functional Polymer) and Irganox 1010 (BASF) were used as received.

*2.2 Synthesis of imine-containing α,ω-diamine cross-linker (**ICL**)*

A solution of terephthalaldehyde (4.00 g, 29.8 mmol) in chloroform (10 mL) was added dropwise to a solution of HMDA (6.93 g, 59.6 mmol) and *p*-TSA (56 mg, 0.30 mmol) in chloroform (10 mL) maintained at 70 °C for 4.5 h. The unreacted HMDA was extracted with water (2 × 50 mL). The organic layer was then dried with anhydrous magnesium sulphate, the solvent was evaporated under vacuum and **ICL** was obtained as a slightly yellow solid (3.30 g, 58.1%). ^{1}H NMR (400 MHz, $CDCl_3$, δ): 8.24 (s, CH_2CH_2N=C**H**, 2H), 7.71 (s, Ar**H**, 4H), 3.59 (t, *J* = 6.6 Hz, $CH_2C\mathbf{H}_2N$=CH, 4H), 2.64 (t, *J* = 6.7 Hz, $(CH_2)_3C\mathbf{H}_2NH_2$, 4H), 1.70 (m, $C\mathbf{H}_2CH_2N$=CH, 4H), 1.42-1.32 (m, $(C\mathbf{H}_2)_3CH_2NH_2$, 12H) ppm. ^{13}C NMR (100 MHz, $CDCl_3$, δ): δ 160.7 (CH_2CH_2N=**C**H, 2C), 138.4 (**C**$_h$, 2C), 128.6 (**C**$_i$, 4C), 62.2 ($CH_2\mathbf{C}H_2N$=CH, 2C), 42.5 ($(CH_2)_2CH_2\mathbf{C}H_2NH_2$, 2C), 34.1 ($(CH_2)_2\mathbf{C}H_2CH_2NH_2$, 2C), 31.2 ($\mathbf{C}H_2CH_2N$=CH, 2C), 27.6-27.1 ($(\mathbf{C}H_2)_2CH_2CH_2NH_2$, 4C).

2.2.1** DP_n calculation for **ICL

The number of repeat units of **ICL** (*n*) was calculated by ^{1}H NMR spectroscopy from the ratio of the integral of the imine signal in the repeat unit at 8.24 ppm ($I_{8.24}$) and the chain-end methylene signal at 2.63 ppm ($I_{2.63}$) according to eq. 1.

$$n = \frac{I_{8.24}/2}{I_{2.63}/4} \quad (1)$$

Consequently, the polymerization degree (DP_n) was calculated using $DP_n = 2n + 1$.

*2.3 Synthesis of 1-(4-(azidomethyl)benzyl)-4-propyl-1H-1,2,3-triazole (**4**)*

CuI.P(OEt)$_3$ (530 mg, 1.50 mmol) was slowly added to a solution of 1,4-bis(azidomethyl)benzene (**1**, 14.0 g, 74.4 mmol), 1-pentyne (5.06 g, 74.4 mmol) and DIPEA (9.61 g, 74.4 mmol) in tetrahydrofuran (200 mL) that was stirred at 35 °C for 72 h. After drying

under vacuum the crude product was purified by column chromatography using a 1:1 mixture of ethyl acetate and petroleum ether to obtain, after evaporation of the solvents, **4** as a colorless liquid (8.65 g, 45.4%). Starting diazide **1** (5.06 g, 36.1%) and bis-1,2,3-triazole **3** (3.40 g, 14.1%) were also recovered. ^{1}H NMR of **3** (400 MHz, $CDCl_3$, δ): 7.24 (m, Ar**H**, 4H), 7.22 (s, NC**H**=C, 2H), 5.48 (s, NC$\mathbf{H}_2$C, 4H), 2.67 (t, *J* = 7.6 Hz, C$\mathbf{H}_2$$CH_2CH_3$, 4H), 1.68 (m, CH_2C$\mathbf{H}_2$$CH_3$, 4H), 0.94 (t, *J* = 7.6 Hz, CH_2CH_2C$\mathbf{H}_3$, 6H). ^{13}C NMR of **3** (100 MHz, $CDCl_3$, δ): 148.7 (NCH=**C**, 2C), 135.4 (**C$_b$**, 2C), 128.4 (**C$_a$**, 4C), 120.6 (N**C**H=C, 2C), 53.3 (N**C**H_2C, 2C), 27.6 (**C**$H_2CH_2CH_3$, 2C), 22.5 (CH_2**C**H_2CH_3, 2C), 13.7 (CH_2CH_2**C**H_3, 2C). HMRS (ESI, *m/z*): $[M + Na]^+$ calculated for $C_{18}H_{24}N_6Na$, 347.1955; found, 347.1955. ^{1}H NMR of **4** (300 MHz, $CDCl_3$, δ): 7.33 (d, *J* = 8.1 Hz, **H$_c$**, 2H), 7.26 (d, *J* = 8.1 Hz **H$_d$**, 2H), 7.22 (s, NC**H**=C, 1H), 5.50 (s, CC$\mathbf{H}_2$N, 2H), 4.35 (s, C$\mathbf{H}_2N_3$, 2H), 2.68 (t, *J* = 7.6 Hz, C$\mathbf{H}_2$$CH_2CH_3$, 2H), 1.67 (m, CH_2C$\mathbf{H}_2$$CH_3$, 2H), 0.95 (t, *J* = 7.3 Hz, CH_2CH_2C$\mathbf{H}_3$, 3H). ^{13}C NMR of **4** (75 MHz, $CDCl_3$, δ): 148.7 (NCH=**C**, 1C), 135.9 (**C$_b$**, 1C), 135.1 (**C**CH_2N, 1C), 128.7 (**C$_c$**, 2C), 128.3 (**C$_d$**, 2C), 120.6 (N**C**H=C**,** 1C), 54.2 (**C**H_2N_3, 1C), 53.5 (C**C**H_2N, 1C), 27.6 (**C**$H_2CH_2CH_3$, 1C), 22.6 (CH_2**C**H_2CH_3, 1C), 13.7 (CH_2CH_2**C**H_3, 1C). HMRS (ESI, *m/z*): $[M + Na]^+$ calculated for $C_{13}H_{16}N_6Na$, 279.1329; found, 279.1331.

*2.4 Synthesis of 1,2,3-triazolium-containing diamine cross-linker (**TCL**)*

A solution of azido-1,2,3-triazole **4** (912 mg, 3.55 mmol) and 1-azido-8-iodooctane **5** (1.00 g, 3.55 mmol) in acetonitrile (3.5 mL) was heated at 80 °C for 55h. PPh_3 (2.14 g, 8.08 mmol) was added, and the mixture was further stirred at room temperature for 24 h, producing a phosphorimide-1,2,3-triazole intermediate **6$_{IPP}$**. Acetonitrile (4.5 mL) and water (0.5 mL) were added, and the mixture was further stirred at room temperature for 24 h. The mixture was then dried under vacuum, water (16 mL) was added and the targeted compound was extracted with ethyl acetate (3 × 150 mL) and dichloromethane (150 mL). The combined organic phases were washed with water (100 mL), dried with anhydrous magnesium sulphate and evaporated to recover **TCL** as a colourless viscous liquid (499 mg, 34.0%). ^{1}H NMR (400 MHz, DMSO-d_6, δ): 8.85 (s, NC**H**=C, 1H), 7.40 (s, Ar**H**, 4H), 5.81 (s, CC$\mathbf{H}_2$N, 2H), 4.52 (t, *J* = 7.2, CH_2C$\mathbf{H}_2$N, 2H), 4.03 (bs, N$\mathbf{H}_2$, 4H), 3.75 (s, CC$\mathbf{H}_2NH_2$, 2H), 2.84 (t, *J* = 7.6, CC$\mathbf{H}_2$$CH_2CH_3$, 2H), 2.69 (t, *J* = 7.6, $(CH_2)_4CH_2$C$\mathbf{H}_2NH_2$, 2H), 1.84 (m, C$\mathbf{H}_2CH_2$N, 2H), 1.68 (m, CCH_2C$\mathbf{H}_2CH_3$, 2H), 1.46 (m, $(CH_2)_4$C$\mathbf{H}_2CH_2NH_2$, 2H), 1.26 (m, (C$\mathbf{H}_2$)$_4CH_2CH_2NH_2$, 8H), 0.97 (t, *J* = 7.2, CCH_2CH_2C$\mathbf{H}_3$, 3H). ^{13}C NMR (100 MHz, DMSO-d_6, δ): 143.9 (N**C**=CH, 1C), 143.0 (NH_2CH_2**C**CH, 1C), 131.4 (NCH_2**C**CH, 1C), 128.6 (NC=**C**H, 1C), 128.2 (NCH_2C**C**H, 1C), 127.9 (NH_2CH_2C**C**H, 1C), 55.8 (N**C**H_2CCH, 1C), 50.3 (CH_2CH_2**C**H_2N, 1C), 44.3

(NH_2**C**H_2CCH, 1C), 40.0-39.0 ((CH_2)$_3$$CH_2$**C**$H_2NH_2$, 1C), 28.2 ((**C**$H_2$)$_3$$CH_2CH_2NH_2$, 3C), 28.0 ($CH_2$**C**$H_2CH_2$N, 1C), 27.6 (($CH_2$)$_3$**C**$H_2CH_2NH_2$, 1C), 25.3 (**C**$H_2CH_2CH_2$N, 1C), 24.2 (**C**$H_2CH_2CH_3$, 1C), 20.0 ($CH_2$**C**$H_2CH_3$, 1C), 13.2 ($CH_2CH_2$**C**$H_3$, 1C). HMRS (ESI, *m/z*): $[M]^+$ calculated for $C_{21}H_{36}N_5$, 358.2965; found, 358.2967.

2.5 Processing and post-processing of PE CANs and XPE

*2.5.1 Processing of **ICAN$_{0.5}$***

PE-*g*-MA (4.0 g, 0.49 mmol of MA) and Irganox (20 mg, 0.5 wt. % according to PE-*g*-MA) were introduced in the Haake MiniLab III micro compounder and processed at 100 rpm for 2 min at 200 °C in order to restore maleic anhydrides potentially hydrolysed during storage. **ICL** (133 mg, 0.28 mmol of amine, [NH_2]/[MA] = 0.56) was then introduced and the recirculation was maintained for 10 min. The obtained material was then hot pressed for 10 min at 200 °C and 200 bar to afford 1 mm thick disks (Ø = 8 or 25 mm) suited for rheological characterization.

*2.5.2 Processing of **TCAN***

PE-*g*-MA (4.5 g, 0.54 mmol of MA) and Irganox (22 mg, 0.5 wt.% according to PE-*g*-MA) were introduced in the Haake MiniLab III micro compounder and maintained for 2 min at 200 °C and 100 rpm. The temperature was then set at 140 °C and a concentrated solution of **TCL** (0.13 g, 0.27 mmol, [NH_2]/[MA] = 0.5) in acetonitrile (0.4 mL) was added. The blend was allowed to recirculate for 40 min to ensure full reaction of MA at this temperature. After flushing it out, **TCAN** was hot pressed for 10 min at 160 °C and 200 bar to afford 1 mm thick disks (Ø = 8 or 25 mm) suited for rheological characterization.

*2.5.3 Synthesis of **XPE***

A non-dynamic PE network was synthesized in order to define the highest gel fraction reachable with PE-*g*-MA. A solution of PE-*g*-MA (1.0 g, 0.12 mmol of MA) and isophorone diamine (IPDA, 10 mg, 0.12 mmol of amine, [NH_2]/[MA] = 1.0) in xylene (1.3 mL) was heated at 140 °C for 24 h in a closed vial. The resulting gel was dried under vacuum at 100 °C for 24 h to afford **XPE**.

2.6 Characterization methods

^{1}H, ^{13}C and ^{31}P NMR spectra were performed on Bruker AV 400, Bruker AV 300 or Jeol ECZ spectrometers in DMSO-d_6 or $CDCl_3$. Fourier Transform infrared (FTIR) spectra were recorded

in transmission mode on hot pressed ~100 μm thick films using a Thermo Scientific Nicolet iS50 FT-IR with 32 scans and a resolution of 4 cm^{-1}. Each spectrum has been acquired between 3500 cm^{-1} and 500 cm^{-1}. For proper comparison between different samples, spectra were normalized to the peak integral between 700 cm^{-1} and 750 cm^{-1} (corresponding to the rocking deformation of PE [48]). Thermogravimetric analysis (TGA) was performed under nitrogen atmosphere using a TGA Q500 (TA Instruments).

2.7 Swelling experiments

Ca. 100-200 mg of polymer (m_0) were immersed in xylene (6 mL) for 24 h at 110 °C. The swollen sample was weighed (m_s) and dried under vacuum at 100 °C for 24 h in order to measure the mass of the remaining insoluble fraction (m_f). The gel fraction (G_f) and the swelling ratio (S_r) were calculated using equations 2 and 3, respectively:

$$G_f = \frac{m_f}{m_0} \times 100 \quad (2)$$

$$S_r = 1 + \rho_s\left(\frac{m_s}{m_f} - 1\right)/\rho_p \quad (3)$$

where ρ_s and ρ_p are the density of xylene (ρ_s = 0.861 g/cm^3) and PE-*g*-MA (ρ_p = 0.95 g/cm^3).

2.8 Rheological characterizations

Discs (8 mm diameter, 1 mm thickness) were punched from melt-pressed plates. Small amplitude oscillatory shear (SAOS) and stress relaxation (SR) experiments were performed on an ARES G2 rotational rheometer with a parallel plate geometry (8 mm diameter) in a convection oven. Each sample was subjected to alternating SAOS and SR (ca. 1 h for each) experiments at temperatures increasing from 160 to 220 °C with 20 °C steps. In SAOS, the angular frequency was varied from 100 to 0.1 rad s^{-1}. All measurements were performed with a strain of 1%, within the linear viscoelastic regime of the measured material, and with a positive normal force to ensure contact between the sample and the geometry. The fitting of the relaxation modulus *G(t)* was performed by using a stretched exponential model described by equation 4:

$$G(t) = G_0 e^{-\left(\frac{t}{\tau^*}\right)^\beta} \quad (4)$$

where G_0 is a constant and β is related to the breadth of distribution of the relaxation times. From this equation, the average relaxation time $<\tau>$ can then be calculated using equation 5:

$$<\tau> = \tau^* \Gamma\left(\frac{1}{\beta}\right)/\beta \quad (5)$$

3 Results and discussion

3.1 Synthesis of imine- and 1,2,3-triazolium-containing diamine cross-linkers

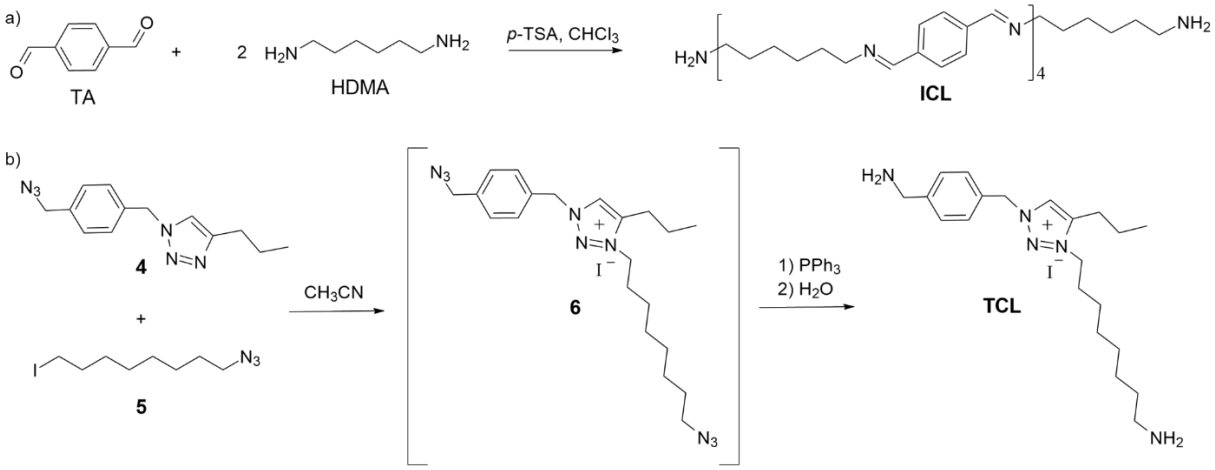

Scheme 1. Syntheses of (a) imine-containing α,ω-diamine cross-linker **ICL** and (b) 1,2,3-triazolium-based diamine cross-linker **TCL**.

Two different diamine cross-linkers containing either imine or 1,2,3-triazolium covalent exchangeable bonds have been considered for the preparation of PE CANs. First, a symmetric α,ω-diamine oligomer containing multiple imine bonds (**ICL**, **Scheme 1a**) was synthesized by AA+BB step growth polycondensation of HMDA and TA adapting a previously reported procedure [49]. The polymerization was catalysed by *p*-TSA (0.005 equiv. according to aldehyde groups) in a 42 wt.% chloroform solution of HDMA and TA [49]. An excess of HMDA was used ([NH_2]/[CHO] = 2.0) in order to yield oligomers with amine-functionalized chain-ends and low DP_n thus ensuring solubility in common organic solvents for characterization purpose and the use of minimal mass of **ICL** for the reactive processing of PE CANs. Such deviation from stoichiometry also leads to unreacted HMDA, which should be removed to prevent the formation of permanent amide cross-links by reaction of HMDA with PE-*g*-MA during processing. Residual HMDA was extracted in water from chloroform as confirmed by ^{1}H NMR spectroscopy with a ca. 4-fold decrease of the signal at 2.63 ppm that corresponds to aminomethylene groups from HMDA and the chain-ends of **ICL** (**Fig. S1**). The chemical structure of **ICL** was confirmed by complete assignment of all ^{1}H and ^{13}C NMR signals (**Fig. S2 and S3**). Besides, ^{1}H NMR spectroscopy demonstrated the absence of aldehyde signal at 9.83 ppm thus confirming the complete conversion of TA and the exclusive presence of amine-functionalized chain-ends. Moreover, the polymerization degree of **ICL** (DP_n = 2n+1

= 9, M_n = 972 g mol^{-1}) could be calculated by comparison of the integrals of the protons from aminomethylene chain-ends and from the imine groups in the repeat units at 2.63 and 8.24 ppm, respectively, assuming a complete extraction of HMDA.

Secondly, a 1,2,3-triazolium-based diamine cross-linker (**TCL**) was synthesized in 3 steps: i) copper(I)-catalyzed 1,3-dipolar cycloaddition between 1,4-bis(azidomethyl)benzene **1** and pent-1-yne **2**, ii) *N*-alkylation of the *N*-3 position of the resulting azide-functionalized 1,2,3-triazole **4** by 1-azido-8-iodooctane **5**, and iii) the Staudinger reduction of the resulting 1,2,3-triazolium-based diazide **6** into the corresponding 1,2,3-triazolium-based diamine cross-linker (**TCL**, **Scheme 1b** and **Scheme S1**). As novel compounds, the purity and chemical structures of **3**, **4** and **TCL** were thoroughly confirmed by full assignment of ^{1}H and ^{13}C NMR spectra (**Fig. 1** and **Fig. S4-S8**) as well as characterization by ESI-HRMS. Several characteristic signals on the ^{1}H NMR spectra of **TCL** and the shifting of their chemical displacements compared to their precursors **4** and **5** could attest the structure and purity of **TCL** as well as the overall efficiency of the developed synthetic route (**Fig. S9**). In particular, quantitative *N*-alkylation of the 1,2,3-triazole group of **4** was confirmed by the appearance of the 1,2,3-triazolium signal at 8.89 ppm, the disappearance of the 1,2,3-triazole group at 7.90 ppm and the downfield shift of the chemical displacements of the methylene signals at the *N*-1, *N*-3 and *C*-4 positions of the 1,2,3-triazolium group (at 5.81, 4.52 and 2.82 ppm, respectively) compared to those of their functional precursors (at 5.55 and 2.57 for azido-1,2,3-triazole **4**, and 3.31 ppm for azido-iodide **5**). Moreover, the completion of the Staudinger reaction is attested by the appearance of the amine protons at 4.03 ppm and the upfield shift of the chemical displacements of the aminomethylene signals (at 3.75 and 2.69 ppm for benzylic and aliphatic methylene groups of **TCL**) compared to those of the azidomethylene groups of the functional precursors (at 4.43 and 3.27 ppm for benzylic and aliphatic methylene groups of **4** and **5**, respectively). Besides, ^{31}P NMR demonstrates the formation of the iminophosphorane intermediate at 8.86 ppm after reaction of **6** with PPh_3 (**6$_{IPP}$**, **Scheme S1**) as well as the total hydrolysis of this intermediate and the efficient removal of all phosphorylated species after **TCL** purification (**Fig. S10**).

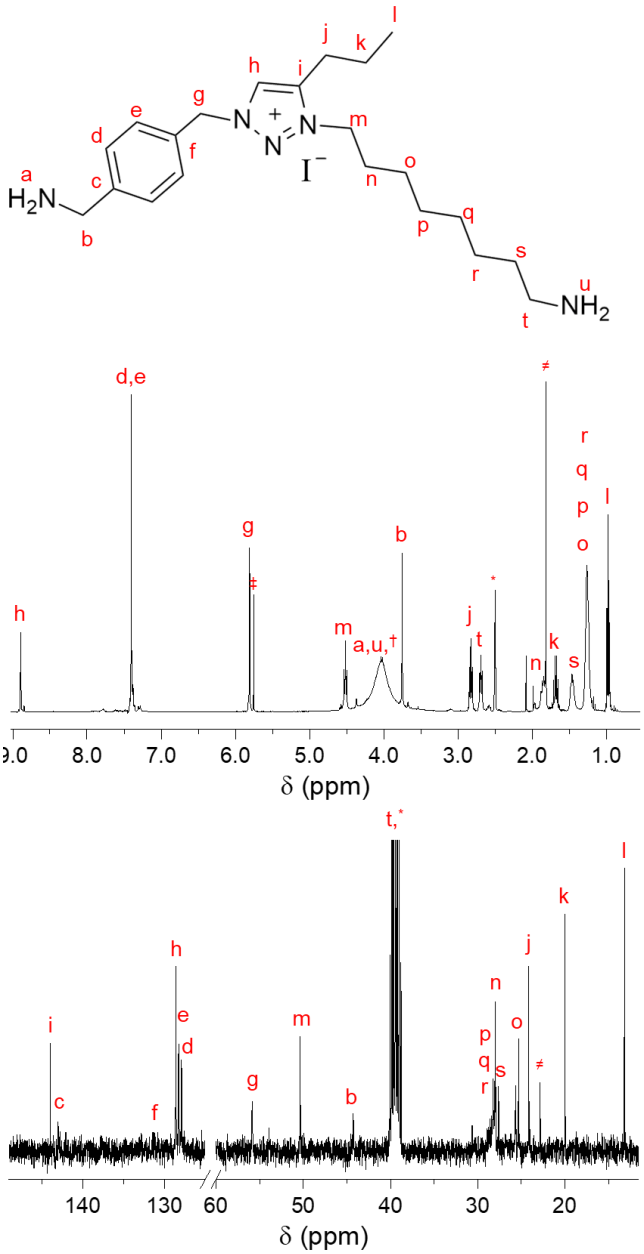

Fig. 1. ^{1}H (top, 400 MHz) and ^{13}C (bottom, 100 MHz) NMR spectra of **TCL** in DMSO-d_6. *: DMSO, †: H_2O, ‡: DCM, $^{\neq}$: acetone.

3.2 Processing and characterization of ***ICAN$_{0.5}$***

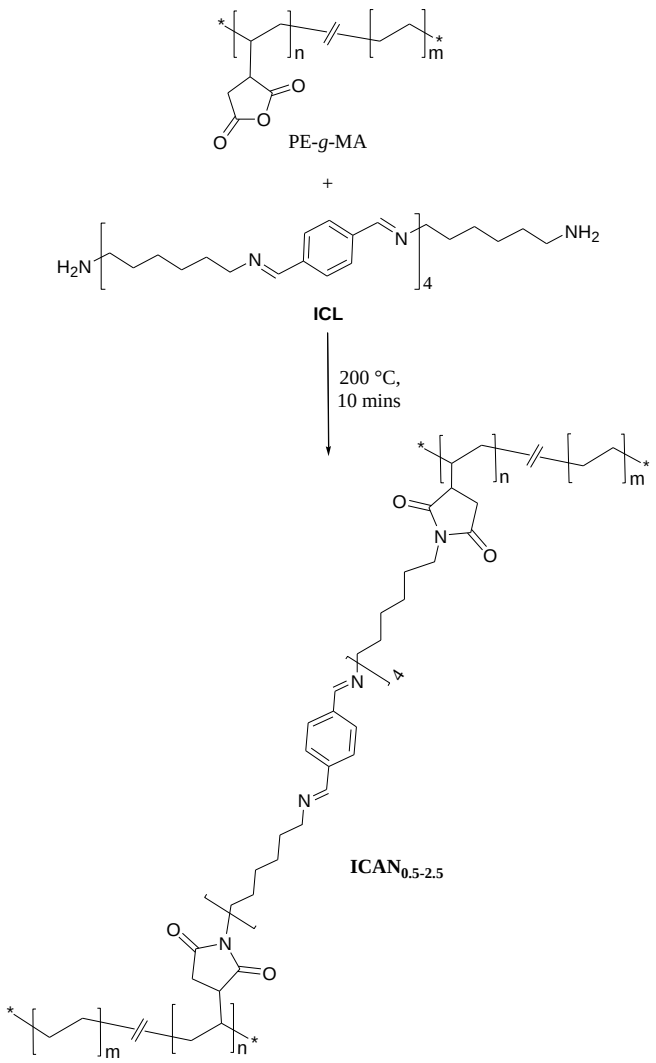

Scheme 2. Synthesis of **ICAN$_{0.5\text{-}2.5}$** by reactive melt processing of **ICL** and PE-*g*-MA.

The two diamine-functionalized cross-linkers carrying several imine bonds (**ICL**) or a single 1,2,3-triazolium group (**TCL**) were further implemented into the melt reactive processing of PE CANs through the reaction of the terminal amines with the pendent maleic anhydrides of PE-*g*-MA. Imine-based PE CANs (**ICAN$_{0.5}$** to **ICAN$_{2.5}$**, **Scheme 2**) were obtained by reactive processing at 200 °C for 10 min using **ICL** and PE-*g*-MA with [NH_2]/[MA] ratios ranging from 0.5 to 2.5 (**Table 1**). While **ICAN$_{0.5}$** is reprocessable by compression moulding at 200 °C for 10 mins (**Figure 2a**, **left**), samples with higher [NH_2]/[MA] ratios could not be compression moulded after the reactive processing step and were thus not considered further. TGA experiments carried out on both the dynamic cross-linkers and the resulting PE CANs confirm

the absence of decomposition during isotherms at 200 °C (**Fig. S11**) and high thermal stabilities with temperatures at 10% weight loss (T_{d10}) up to 280 °C for the cross-linkers and 420 °C for the PE CANs **(Fig. S12)**.

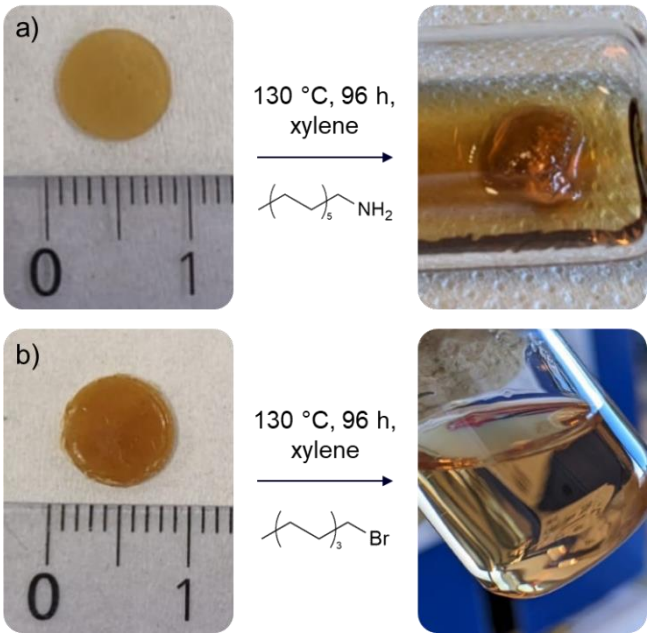

Fig. 2. Digital images of (a) **ICAN$_{0.5}$** and (b) **TCAN** after compression molding (left) and after reactive dissolution tests (right).

FTIR spectroscopy of **ICAN$_{0.5}$** (**Fig. 3**) proved the occurrence of the targeted reaction between amine and anhydride groups with the consequent appearance of the C=O stretching band of imide groups at 1710 cm^{-1} [32]. However, the almost total disappearance of the C=O stretching bands at 1790 and 1865 cm^{-1} of PE-*g*-MA anhydride groups was unexpected due to the initial two-fold excess of anhydrides compared to amines [50]. Besides, the absence of the imine stretching band at 1645 cm^{-1}, well visible for **ICL**, indicates extensive dissociation of the imine bonds during processing. Both results are consistent with the depolymerisation of **ICL** oligomers into HMDA and TA, followed by immediate reaction of HMDA with anhydride groups. Such reaction normally proceeds in presence of water but as water is also generated during the condensation of amines and anhydrides into imides, a catalytic amount might suffice. Also, another consequence of such undesired reaction would be the formation of non-dynamic imide covalent cross-links. This hypothesis was confirmed by measuring the G_f of **ICAN$_{0.5}$** (24 h at 140 °C in xylene), which amounts to 51% (with a swelling ratio of 12.9). For comparison, a fully non-dynamic covalently cross-linked PE network (**XPE**) obtained by reaction between PE-*g*-MA and IPDA (with [NH$_2$]/[MA] = 1.0) exhibited G_f of 62% (with a swelling ratio of

14.4). Moreover, the swelling of **ICAN$_{0.5}$** in a reactive solution of dodecylamine in xylene at 130 °C for 96 h, also yields a monolithic gel, thus confirming a predominance of non-dynamic and non-cleavable cross-links (**Fig. 2a right**).

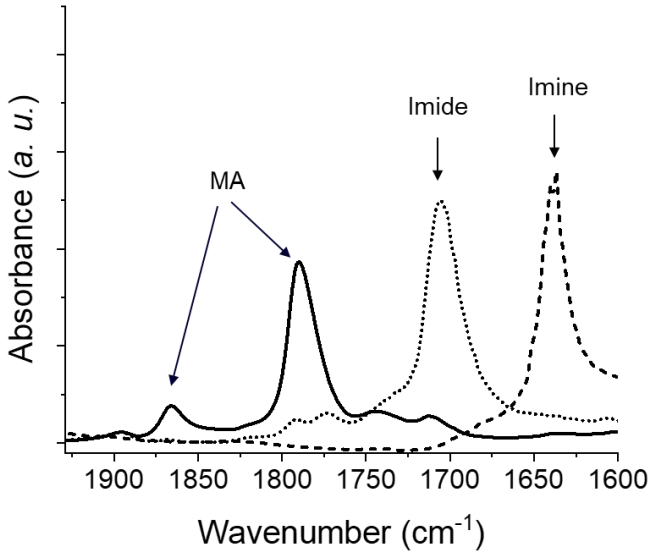

Fig. 3. FTIR spectra of carbonyls region of dried PE-*g*-MA (solid line), **ICAN$_{0.5}$** (dotted line) and **ICL** (dashed line) from 1950 to 1600 cm^{-1}.

Table 1. Formulation and properties of cross-linked PE networks.

Sample	Cross-linker	[NH_2]/[MA]	G_f[a] (%)	S_r[b]	*G* at 10 s (200 °C), (MPa)[c]
ICAN$_{0.5}$	**ICL**	0.5	51	12.9	1.1
TCAN	**TCL**	1.0	31	23.5	0.15
XPE	**IPDA**	1.0	62	14.4	-

[a]Gel fraction calculated using *eq. 2;* [b]Swelling ratio calculated using *eq. 3*; [c]Network modulus determined from rheological stress relaxation.

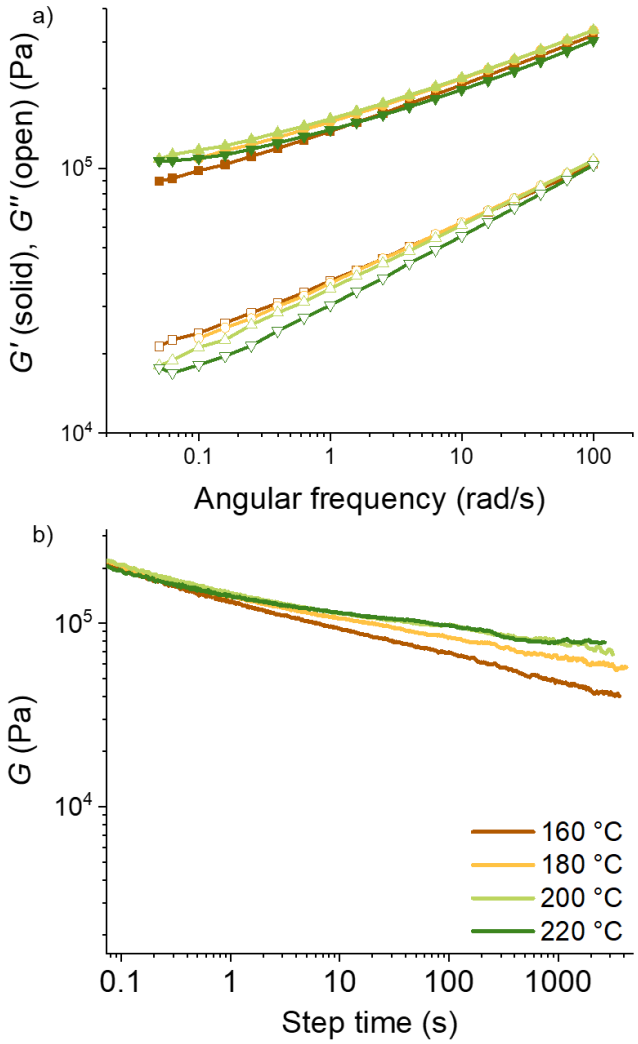

Fig. 4. SAOS (a) and stress relaxation (b) of **ICAN$_{0.5}$** performed at 1% deformation at increasing temperatures.

The rheological properties of **ICAN$_{0.5}$** were then investigated by performing SAOS (**Fig. 4a**) followed by stress relaxation experiments (**Fig. 4b**) at temperatures in the 160-220 °C range. All experiments have been run on the same sample by increasing successively the temperatures. While this process leads to prolonged heating of the sample, it also guarantees that the effective contact between the geometries and the sample does not affect the measurements. Given the PE backbone of these networks with T_g far below measurement temperature, the upturn of *G*' and *G*'' at high frequencies denotes a relaxation from the entangled state spreading over a wide range of frequencies. This might originate from the presence of highly defective network structure with dangling chains and sol fraction in accordance with the low G_f (51 %), but also from partial relaxation of imide cross-links. At low frequencies, the premises of a plateau

indicate formation of a cross-linked structure. The corresponding relaxation moduli show plateaus at long times, indicating the presence of permanent cross-links. The plateau moduli appear to increase when probing successively the same sample at increased temperatures, reaching 80 kPa at 220 °C (at t = 1000 s). This is due to further formation of non-dynamic cross-links consequent to imine dissociation and reaction of released diamines with residual anhydrides during extended thermal annealing. In conclusion, the reactive processing of **ICL** with PE-*g*-MA afforded PE networks with relatively high G_f. However, the lack of chemical degradability and the absence of complete stress relaxation points toward the formation of non-dynamic cross-links. We attributed those to the depolymerisation of **ICL** at high temperatures during the processing step, quickly followed by reaction of HMDA with pendent maleic anhydrides forming permanent cross-links.

*3.3 Processing and characterization of **TCAN***

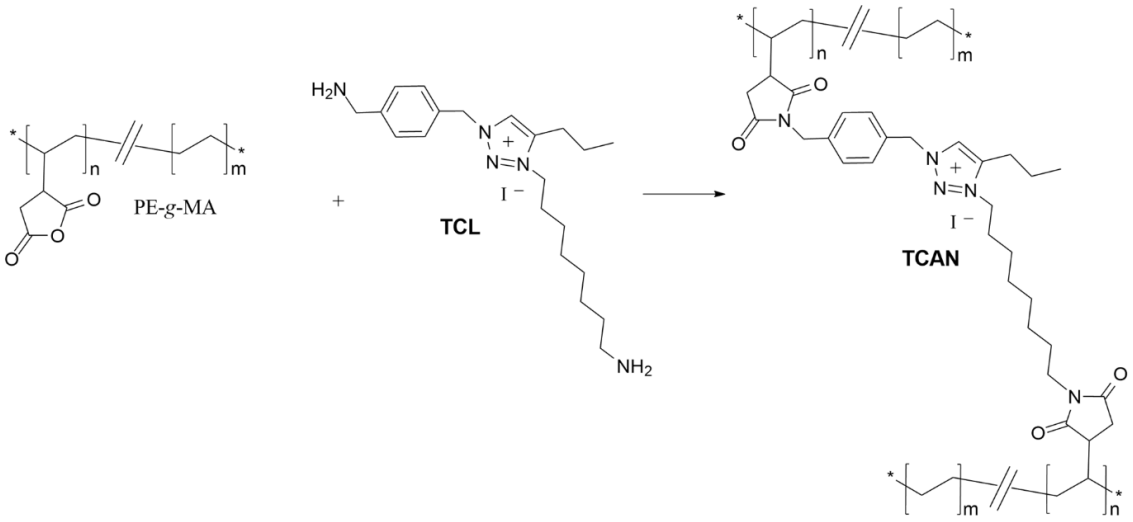

Scheme 3. Synthesis of **TCAN** by reactive melt processing of **TCL** and PE-*g*-MA.

1,2,3-Triazolium-based PE CAN (**TCAN**) was obtained by reactive processing in the melt at 200 °C for 40 min of **TCL** and PE-*g*-MA with an initial [NH_2]/[MA] ratio of 1.0 (**Table 1**). As for **ICAN$_{0.5}$**, the synthesis relies on the reaction between pendent maleic anhydrides of PE-*g*-MA with the amine groups of the dynamic cross-linker that contains a single 1,2,3-triazolium group (**Scheme 3**). Conversely to **ICAN$_{0.5}$**, the use of a [NH_2]/[MA] ratio of 1.0 afforded a material that could be easily re-processed by compression moulding at 160 °C after the processing step, suggesting that the material involves dynamic cross-links.

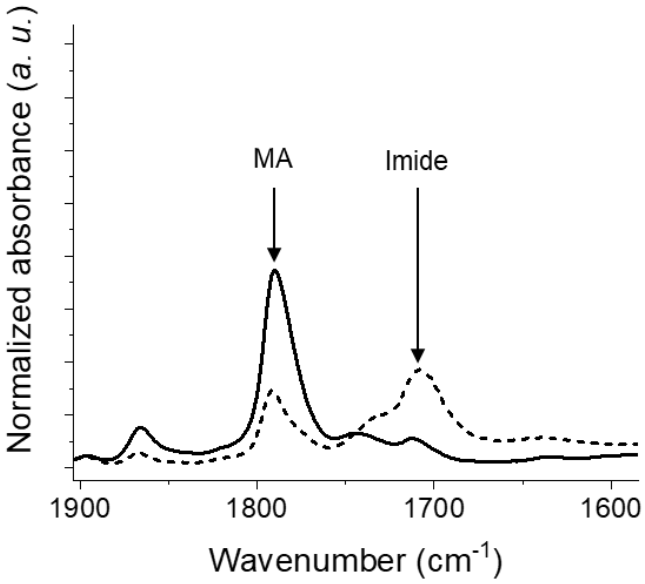

Fig. 5. FTIR spectra of **TCAN** (dashed line) and dry PE-*g*-MA (solid line).

FTIR characterization of **TCAN** (**Fig. 5**) shows the formation of imide bonds at 1710 cm^{-1} expected from reaction of amine groups with maleic anhydrides. However, although a stoichiometric amount of amine and anhydride functionalities were used, the C=O stretching bands of MA groups at 1790 and 1865 cm^{-1} do not completely disappear and the intensity of the band associated to imide groups is lower than for **ICAN$_{0.5}$**. The lower grafting efficiency was also verified by swelling experiments that displayed a lower gel fraction for **TCAN** than for **XPE** (G_f = 31 and 62%; S_r = 23.5 and 14.4, respectively). This difference may indicate a loss of primary amine functionalities from the **TCL** cross-linker during the formation of the network most likely resulting from undesirable side-reactions occurring at the initial processing stage. At such high temperatures, 1,2,3-triazolium halides are indeed known to undergo fast reversible de-*N*-alkylation equilibrium yielding alkyl halides and 1,2,3-triazoles. Concurrent re-*N*-alkylation involving alkyl halides with far more reactive primary amines may lead to the formation of ammonium halide by-products. A likely overall mechanism is presented in **Scheme 4**. De-*N*-alkylation of **TCL** prior to its reaction with maleimide groups to yield dynamic 1,2,3-triazolium cross-links (**Scheme 4a**) leads to iodide- and 1,2,3-triazole-functionalized primary amines (**Scheme 4b**). Such amines may undergo reaction with maleic anhydrides from PE-*g*-MA to yield 1,2,3-triazole- and iodide-functionalized dangling chains (**Scheme 4c**) and be further involved in trans-*N*-alkylation exchanges of 1,2,3-triazolium cross-links (**Scheme 4d**). Besides, iodide-functionalized primary amines can also self-react through an AB+AB polyaddition mechanism to yield α-iodide,ω-amine ammonium-based ionenes

(**Scheme 4e**) [51]. These ionenes can react with maleic anhydrides from PE-*g*-MA yielding halide-functionalized dangling chains (**Scheme 4f**) and be further involved in trans-*N*-alkylation exchanges through their reaction with 1,2,3-triazole-functionalized dangling chains to yield alternative 1,2,3-triazolium cross-links (**Scheme 4g**). Therefore, mainly three distinct chemical entities might be grafted on the PE backbones: i) 1,2,3-triazolium cross-links originating from **TCL**, ii) 1,2,3-triazolium cross-links incorporating ammonium iodide segments, and iii) 1,2,3-triazole dangling chains. In all cases, reaction of primary amines with iodides should result in i) an overall loss of amine functionalities, ii) an imbalance between iodide- and 1,2,3-triazole-functionalized dangling chains, and therefore iii) an overall decrease in cross-link density. This is indeed consistent with unreacted anhydride groups observed by FTIR and lower cross-link density inferred from swelling experiments. It is worth noting that ammonium groups might also be involved in dissociative exchanges (**Scheme S2**), although exchange rates have not been reported [52].

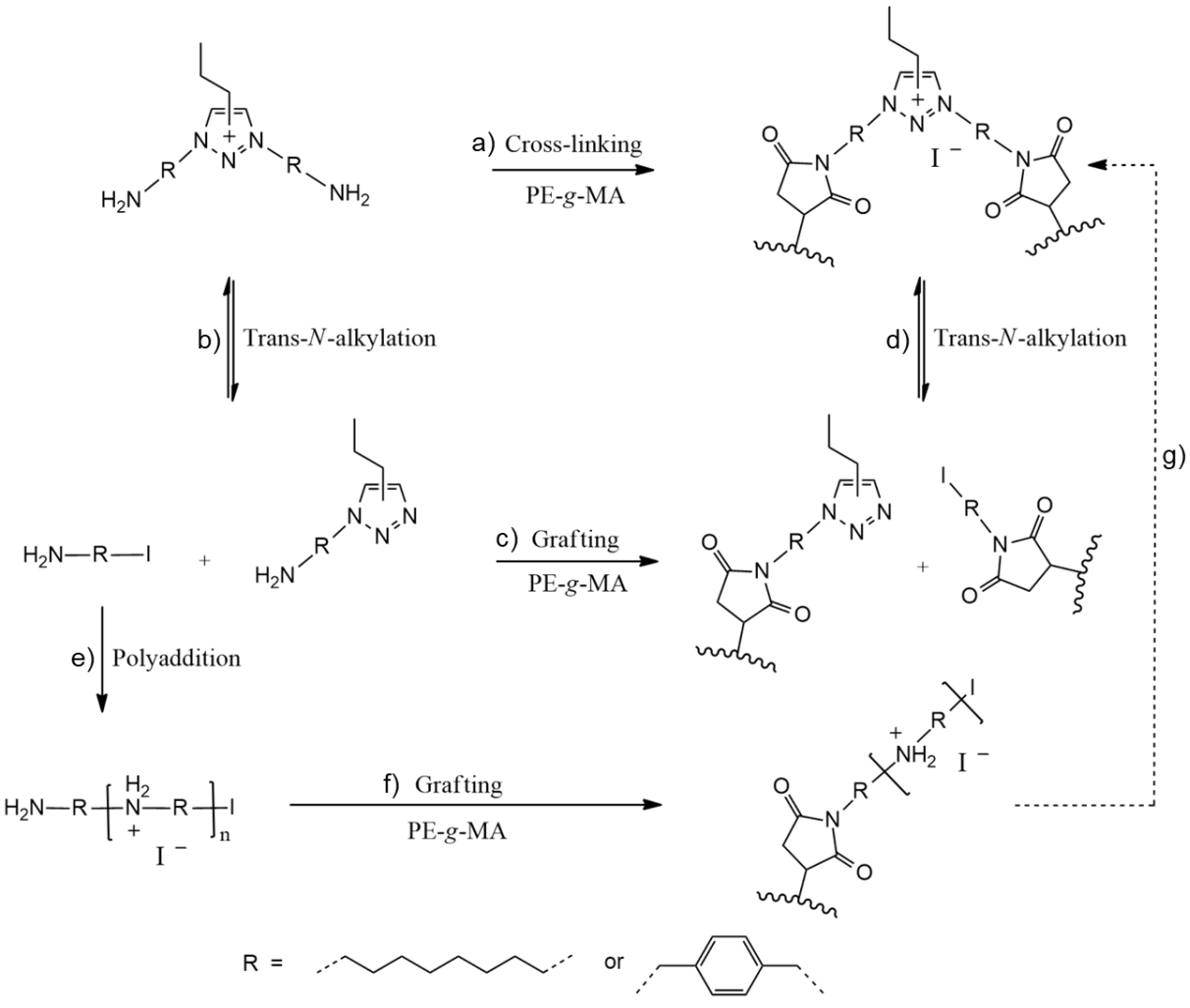

Scheme 4. Chemical reactions occurring during the melt reactive processing of **TCL** and PE-*g*-MA. a) cross-linking by condensation of amines from **TCL** and MA from PE-*g*-MA. b) Trans-*N*-alkylation of molecular diamine-functionalized 1,2,3-triazoliums. c) Grafting of amine-functionalized iodides and 1,2,3-triazoles by condensation reaction with MA forming iodide- and 1,2,3-triazole-functionalized dangling chains. d) Trans-*N*-alkylation of 1,2,3-triazolium cross-links. e) Polyaddition of α-iodide,ω-amines forming ammonium iodide-based ionenes. f) Grafting of α-iodide,ω-amine-functionalized ionenes with MA forming iodide-functionalized ammonium-based ionene dangling chains. g) Insertion of iodide-functionalized ammonium-based ionene dangling chains in trans-*N*-alkylation exchanges of 1,2,3-triazolium cross-links.

The dynamic nature of the obtained **TCAN** was investigated by reactive dissolution and rheological experiments. Immersion into a reactive solution of octyl bromide in xylene for 96 h at 130 °C leads to complete dissolution of **TCAN** (**Fig. 3b**). This is consistent with occurrence of trans-*N*-alkylation reactions and confirms that conversely to **ICAN$_{0.5}$** where side reactions afforded non-dynamic cross-links, all cross-links involved in **TCAN** are dynamic.

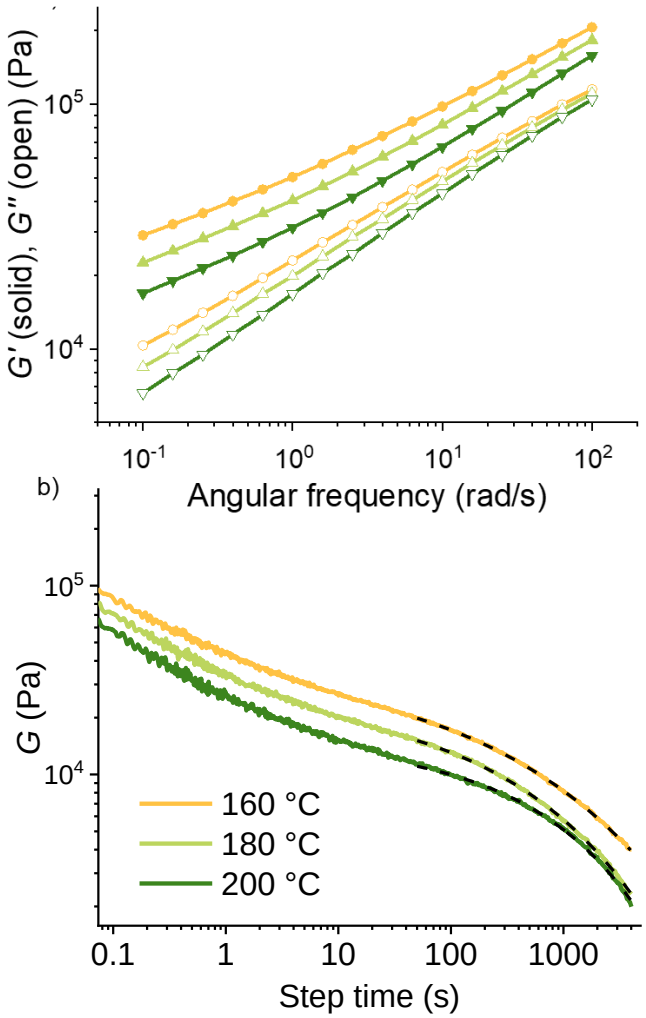

Fig. 6. Frequency sweep (a) and stress relaxation (b) of **TCAN** at increasing temperatures, with corresponding fits using stretched exponentials (dashed lines).

SAOS data carried out at different temperatures (**Fig. 6a**) also indicates large amount of network defects through the upturn of *G*' and *G*'' at high frequencies. The decrease of *G*' plateau values at higher temperatures, also confirmed by stress relaxation data is consistent with a dissociative behaviour. In accordance with swelling data, **TCAN** networks exhibit significantly lower cross-link density than **ICAN$_{0.5}$**, with plateau values ranging between 10 to 30 kPa vs. 100 kPa. **TCAN** display however clear relaxations at longer times (**Fig. 6b**). The corresponding averaged relaxation times (<τ>) obtained by fitting the experimental data with a stretched exponential decay (**Table S1**) decrease from 2900 to 1770 s when increasing the temperature from 160 to 180 °C. First, it is striking to note that these **TCAN** from entangled polymers feature relaxation times up to 60 times higher than networks containing the same 1,2,3-triazolium exchangeable units featuring mixed benzylic and aliphatic substituents at the *N*-1 and *N*-3 positions, yet built from small polyfunctional molecules [45]. Then, a further increase of <τ> to 2480 s at 200 °C suggests that side reactions occur, but without leading to permanent cross-linking in this case. The slowing down of exchange kinetics at high temperatures for **TCAN** most likely result from the rearrangement of *N*-substituents (**Scheme 5**). Indeed, de-*N*-alkylation of the *N*-1 or *N*-3 substituents gives complementary dangling-chains (i.e. benzylic iodide/aliphatic 1,2,3-triazole or aliphatic iodide/benzylic 1,2,3-triazole, respectively) that can further undergo cross-coupling *N*-alkylation reactions to progressively yield a 1:1 mixture of 1,2,3-triazolium cross-links having either two aliphatic or two benzylic *N*-substituents. The exchange kinetics are then governed by the exchange rate of the slower aliphatic/aliphatic cross-links. The previously mentioned ammonium-based cross-links or dangling chains (**Scheme 4** and **S3**) can also compete with trans-*N*-alkylation exchanges of 1,2,3-triazolium groups yielding even slower exchange kinetics.

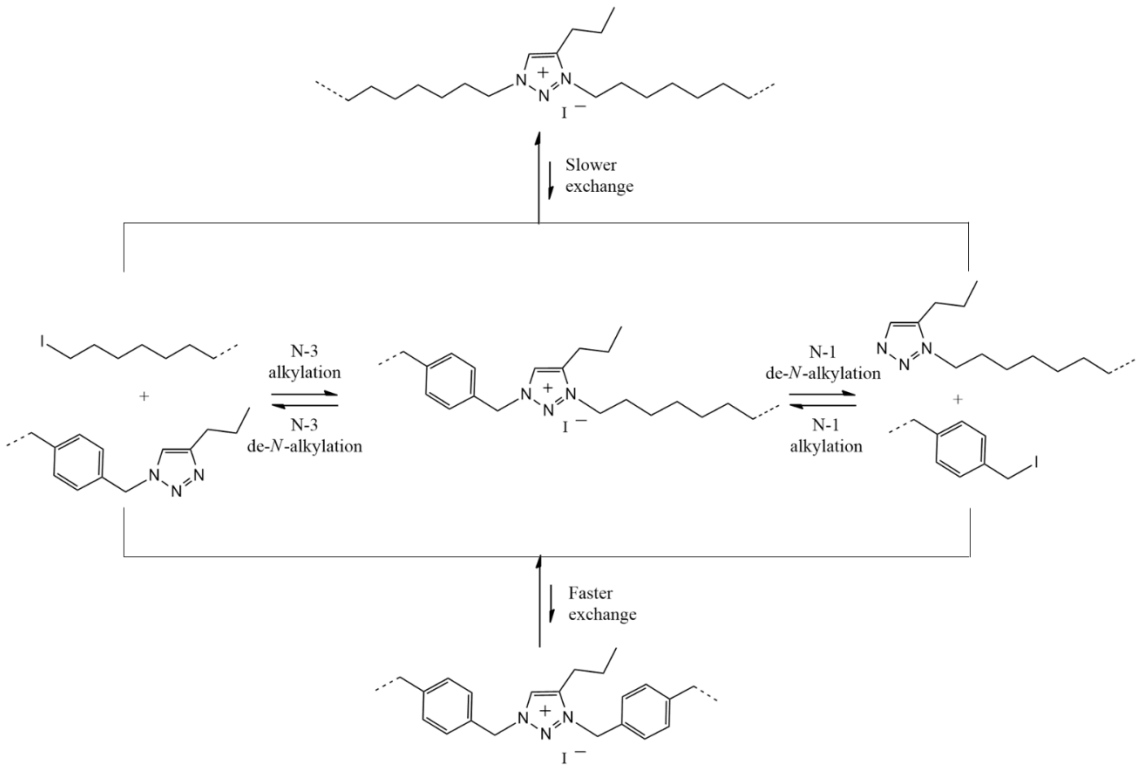

Scheme 5. Aliphatic/aliphatic and benzylic/benzylic 1,2,3-triazolium adducts resulting from cross-coupling *N*-alkylation reactions between iodide- and 1,2,3-triazole dangling chains obtained by de-*N*-alkylation reactions occurring at the *N*-1 and *N*-3 positions.

4 Conclusions

Two diamines carrying exchangeable covalent bonds were successfully synthesized and implemented as dynamic cross-linkers for melt reactive processing of PE CANs using commercially available entangled PE-*g*-MA. While the imine are known to feature very fast exchanges, their incorporation into PE CANs in the form of bis amine cross-linkers lead to side reactions resulting in the formation of a partially permanent network as demonstrated by the lack of chemical degradability and rheological experiments. In contrast incorporation of fast-exchangeable 1,2,3-triazolium cross-links through the same route lead to fully degradable and dynamic networks. Yet, such networks feature relaxation times much slower than networks from small polyfunctional molecules and are not exempt from side reactions either, and demonstrate relatively low G_f as well as evolution of network dynamics at high temperatures suggesting reorganization of 1,2,3-triazolium substituents. This work underlines the challenges involved in the synthesis of entangled PE CANs even when using well established, fast dynamic

chemistries. Grafting dynamic cross-linkers on polyolefins requires highly reactive chemistries capable of C-H activation. A two-step process introducing first a more accessible functionality such as maleic anhydride is well mastered at industrial scale and seems thus appealing. The second grafting step based on amine functional cross-linkers appears however particularly difficult to control, and prone to interfere with many dynamic chemistries used so far.

CRediT authorship contribution statement

Rigatelli Benedetta: Investigation, Writing. Damien Montarnal: Conceptualization, Discussion, Supervision, Writing – review and editing. Eric Drockenmuller: Founding acquisition, Conceptualization, Discussion, Supervision, Writing – review and editing.

Declaration of competing interest

The authors declare that they have no known competing financial interests or personal relationships that could have appeared to influence the work reported in this paper.

Acknowledgements

This project has received funding from the European Union's Horizon 2020 research and innovation programme under the Marie Skłodowska-Curie grant agreement No 860911.

Appendix A. Supplementary data

Supplementary data to this article can be found online at …

References

[1] M. Guerre, C. Taplan, J. M. Winne, and F. E. Du Prez, "Vitrimers: directing chemical reactivity to control material properties," *Chem. Sci.*, vol. 11, no. 19, pp. 4855–4870, 2020, doi: 10.1039/d0sc01069c.

[2] W. Denissen, J. M. Winne, and F. E. Du Prez, "Vitrimers: Permanent organic networks with glass-like fluidity," *Chem. Sci.*, vol. 7, no. 1, pp. 30–38, 2016, doi: 10.1039/c5sc02223a.

[3] V. Concept and M. Hayashi, "Implantation of Recyclability and Healability into Cross-Linked Commercial Polymers by Applying the Vitrimer Concept," *Polymers*, vol. 12, pp. 1–25, 2020.

[4] C. N. Bowman and C. J. Kloxin, "Covalent adaptable networks: Reversible bond structures incorporated in polymer networks," *Angew. Chemie - Int. Ed.*, vol. 51, no. 18, pp. 4272–4274, 2012, doi: 10.1002/anie.201200708.

[5] C. J. Kloxin, T. F. Scott, B. J. Adzima, and C. N. Bowman, "Covalent adaptable networks (CANs): A unique paradigm in cross-linked polymers," *Macromolecules*, vol. 43, no. 6, pp. 2643–2653, 2010, doi: 10.1021/ma902596s.

[6] G. M. Scheutz, J. J. Lessard, M. B. Sims, and B. S. Sumerlin, “Adaptable Crosslinks in Polymeric Materials: Resolving the Intersection of Thermoplastics and Thermosets,” *J. Am. Chem. Soc.*, vol. 141, no. 41, pp. 16181–16196, 2019, doi: 10.1021/jacs.9b07922.

[7] B. R. Elling and W. R. Dichtel, “Reprocessable Cross-Linked Polymer Networks: Are Associative Exchange Mechanisms Desirable?,” *ACS Cent. Sci.*, vol. 6, no. 9, pp. 1488–1496, 2020, doi: 10.1021/acscentsci.0c00567.

[8] D. Montarnal, M. Capelot, F. Tournilhac, and L. Leibler, “Silica-like malleable materials from permanent organic networks,” *Science*, vol. 334, no. 6058, pp. 965–968, 2011, doi: 10.1126/science.1212648.

[9] C. Bowman, F. Du Prez, and J. Kalow, “Introduction to chemistry for covalent adaptable networks,” *Polym. Chem.*, vol. 11, no. 33, pp. 5295–5296, 2020, doi: 10.1039/d0py90102d.

[10] M. Podgórski *et al.*, “Toward Stimuli-Responsive Dynamic Thermosets through Continuous Development and Improvements in Covalent Adaptable Networks (CANs),” *Adv. Mater.*, vol. 32, no. 20, pp. 1–26, 2020, doi: 10.1002/adma.201906876.

[11] L. Leibler, M. Rubinstein, and R. H. Colby, “Dynamics of Reversible Networks,” *Macromolecules*, vol. 24, no. 16, pp. 4701–4707, 1991, doi: 10.1021/ma00016a034.

[12] J. J. Lessard, K. A. Stewart, and B. S. Sumerlin, “Controlling Dynamics of Associative Networks through Primary Chain Length,” *Macromolecules*, vol. 55, no. 22, pp. 10052–10061, 2022, doi: 10.1021/acs.macromol.2c01909.

[13] M. Ahmadi, A. Hanifpour, S. Ghiassinejad, and E. Van Ruymbeke, “Polyolefins Vitrimers : Design Principles and Applications,” *Chem. Mater.*, vol. 34, p. 10249−10271, 2022, doi: 10.1021/acs.chemmater.2c02853.

[14] M. Röttger, T. Domenech, R. Van Der Weegen, A. Breuillac, R. Nicolaÿ, and L. Leibler, “High-performance vitrimers from commodity thermoplastics through dioxaborolane metathesis,” *Science*, vol. 356, no. 6333, pp. 62–65, 2017, doi: 10.1126/science.aah5281.

[15] L. M. Peng *et al.*, “Leakage-Proof and Malleable Polyethylene Wax Vitrimer Phase Change Materials for Thermal Interface Management,” *ACS Appl. Energy Mater.*, vol. 4, no. 10, pp. 11173–11182, 2021, doi: 10.1021/acsaem.1c02052.

[16] W. Y. Wang *et al.*, “Vitrimers of polyolefin elastomer with physically cross-linked network,” *J. Polym. Res.*, vol. 28, no. 210, pp. 1–11, 2021, doi: 10.1007/s10965-021-02573-3.

[17] M. Maaz, A. Riba-Bremerch, C. Guibert, N. J. Van Zee, and R. Nicolaÿ, “Synthesis of Polyethylene Vitrimers in a Single Step: Consequences of Graft Structure, Reactive Extrusion Conditions, and Processing Aids,” *Macromolecules*, vol. 54, no. 5, pp. 2213–2225, 2021, doi: 10.1021/acs.macromol.0c02649.

[18] F. Caffy and R. Nicolaÿ, “Transformation of polyethylene into a vitrimer by nitroxide radical coupling of a bis-dioxaborolane,” *Polym. Chem.*, vol. 10, no. 23, pp. 3107–3115, 2019, doi: 10.1039/c9py00253g.

[19] L. M. Fenimore, B. Chen, and J. M. Torkelson, “Simple upcycling of virgin and waste polyethylene into covalent adaptable networks: catalyst-free, radical-based reactive processing with dialkylamino disulfide bonds,” *J. Mater. Chem. A*, vol. 10, no. 46, pp.

24726–24745, 2022, doi: 10.1039/d2ta06364f.

[20] L. M. Fenimore *et al.*, “Covalent adaptable networks and thermosets of multi-block ethylene/1-octene copolymers made by free-radical processing: Effects of melt flow index and crystallinity on thermomechanical properties and reprocessability,” *Eur. Polym. J.*, vol. 202, p. 112661, 2024, doi: 10.1016/j.eurpolymj.2023.112661.

[21] A. Takahashi, R. Goseki, and H. Otsuka, “Thermally Adjustable Dynamic Disulfide Linkages Mediated by Highly Air-Stable 2,2,6,6-Tetramethylpiperidine-1-sulfanyl (TEMPS) Radicals,” *Angew. Chemie - Int. Ed.*, vol. 56, no. 8, pp. 2016–2021, 2017, doi: 10.1002/anie.201611049.

[22] G. P. Kar, M. O. Saed, and E. M. Terentjev, “Scalable upcycling of thermoplastic polyolefins into vitrimers through transesterification,” *J. Mater. Chem. A*, vol. 8, no. 45, pp. 24137–24147, 2020, doi: 10.1039/d0ta07339c.

[23] S. Wang *et al.*, “Upcycling of post-consumer polyolefin plastics to covalent adaptable networks via in situ continuous extrusion cross-linking,” *Green Chem.*, vol. 23, no. 8, pp. 2931–2937, 2021, doi: 10.1039/d0gc04337k.

[24] M. O. Saed, X. Lin, and E. M. Terentjev, “Dynamic Semicrystalline Networks of Polypropylene with Thiol-Anhydride Exchangeable Crosslinks,” *ACS Appl. Mater. Interfaces*, vol. 13, no. 35, pp. 42044–42051, 2021, doi: 10.1021/acsami.1c12099.

[25] M. C. Montoya-ospina, X. Tan, and T. A. Osswald, “Effect of cross-linking on the mechanical properties, degree of crystallinity and thermal stability of polyethylene vitrimers,” *SPE Polym. Eng. Sci.*, pp. 1–11, 2022, doi: 10.1002/pen.26178.

[26] M. C. Montoya-ospina, “Processing and rheological behavior of cross-linked polyethylene containing disulfide bonds,” *SPE Polym.*, pp. 1–16, 2021, doi: 10.1002/pls2.10062.

[27] F. Ji, X. Liu, C. Lin, Y. Zhou, L. Dong, and S. Xu, “Reprocessable and Recyclable Crosslinked Polyethylene with Triple Shape Memory Effect,” *Macromol. Mater. Eng.*, vol. 1800528, pp. 1–8, 2019, doi: 10.1002/mame.201800528.

[28] J. Tellers, R. Pinalli, M. Soliman, J. Vachon, and E. Dalcanale, “Reprocessable vinylogous urethane cross-linked polyethylene via reactive extrusion,” *Polym. Chem.*, vol. 10, pp. 5534–5542, 2019, doi: 10.1039/c9py01194c.

[29] A. Zych, R. Pinalli, M. Soliman, J. Vachon, and E. Dalcanale, “Polyethylene vitrimers via silyl ether exchange reaction,” *Polymer*, vol. 199, p. 122567, 2020, doi: 10.1016/j.polymer.2020.122567.

[30] F. Yang, L. Pan, Z. Ma, Y. Lou, Y. Li, and Y. Li, “Highly elastic, strong, and reprocessable cross-linked polyolefin elastomers enabled by boronic ester bonds,” *Polym. Chem.*, vol. 11, no. 19, pp. 3285–3295, 2020, doi: 10.1039/d0py00235f.

[31] L. Cheng, B. Li, S. Liu, and W. Yu, “Vitrimer bead foams: Cell density control by cell splitting in weld-compression molding,” *Polymer*, vol. 232, p. 124159, 2021, doi: 10.1016/j.polymer.2021.124159.

[32] Z. He, H. Niu, L. Liu, S. Xie, Z. Hua, and Y. Li, “Elastomeric polyolefin vitrimer: Dynamic imine bond cross-linked ethylene/propylene copolymer,” *Polymer*, vol. 229, p. 124015, 2021, doi: 10.1016/j.polymer.2021.124015.

[33] R. L. Snyder, C. A. L. Lidston, G. X. De Hoe, M. J. S. Parvulescu, M. A. Hillmyer, and G. W. Coates, “Mechanically robust and reprocessable imine exchange networks from modular polyester pre-polymers,” *Polym. Chem.*, vol. 11, no. 33, pp. 5346–5355, 2020, doi: 10.1039/c9py01957j.

[34] X. Liu, L. Liang, M. Lu, X. Song, H. Liu, and G. Chen, “Water-resistant bio-based vitrimers based on dynamic imine bonds: Self-healability, remodelability and ecofriendly recyclability,” *Polymer*, vol. 210, p. 123030, 2020, doi: 10.1016/j.polymer.2020.123030.

[35] P. Taynton, K. Yu, R. K. Shoemaker, Y. Jin, H. J. Qi, and W. Zhang, “Heat- or water-driven malleability in a highly recyclable covalent network polymer,” *Adv. Mater.*, vol. 26, no. 23, pp. 3938–3942, 2014, doi: 10.1002/adma.201400317.

[36] Z. Zhou, X. Su, J. Liu, and R. Liu, “Synthesis of Vanillin-Based Polyimine Vitrimers with Excellent Reprocessability, Fast Chemical Degradability, and Adhesion,” *ACS Appl. Polym. Mater.*, vol. 2, no. 12, pp. 5716–5725, 2020, doi: 10.1021/acsapm.0c01008.

[37] P. Taynton *et al.*, “Re-healable polyimine thermosets: Polymer composition and moisture sensitivity,” *Polym. Chem.*, vol. 7, no. 46, pp. 7052–7056, 2016, doi: 10.1039/c6py01395c.

[38] M. Ciaccia and S. Di Stefano, “Mechanisms of imine exchange reactions in organic solvents,” *Org. Biomol. Chem.*, vol. 13, no. 3, pp. 646–654, 2015, doi: 10.1039/c4ob02110j.

[39] C. D. Meyer, C. S. Joiner, and J. F. Stoddart, “Template-directed synthesis employing reversible imine bond formation,” *Chem. Soc. Rev.*, vol. 36, no. 11, pp. 1705–1723, 2007, doi: 10.1039/b513441m.

[40] M. Ciaccia, R. Cacciapaglia, P. Mencarelli, L. Mandolini, and S. Di Stefano, “Fast transimination in organic solvents in the absence of proton and metal catalysts. A key to imine metathesis catalyzed by primary amines under mild conditions,” *Chem. Sci.*, vol. 4, no. 5, pp. 2253–2261, 2013, doi: 10.1039/c3sc50277e.

[41] M. M. Obadia, B. P. Mudraboyina, A. Serghei, D. Montarnal, and E. Drockenmuller, “Reprocessing and Recycling of Highly Cross-Linked Ion-Conducting Networks through Transalkylation Exchanges of C − N Bonds,” *J. Am. Chem. Soc.*, vol. 137, pp. 6078–6083, 2015, doi: 10.1021/jacs.5b02653.

[42] I. Abdelhedi-Miladi, M. M. Obadia, I. Allaoua, A. Serghei, H. Ben Romdhane, and E. Drockenmuller, “1,2,3-Triazolium-Based Poly(Ionic Liquid)S Obtained Through Click Chemistry Polyaddition,” *Macromol. Chem. Phys.*, vol. 215, no. 22, pp. 2229–2236, 2014, doi: 10.1002/macp.201400182.

[43] M. M. Obadia and E. Drockenmuller, “Poly(1,2,3-triazolium)s: A new class of functional polymer electrolytes,” *Chem. Commun.*, vol. 52, no. 12, pp. 2433–2450, 2016, doi: 10.1039/c5cc09861k.

[44] R. Akacha, I. Abdelhedi-Miladi, D. Montarnal, H. Ben Romdhane, and E. Drockenmuller, “Trans-N-alkylation Covalent Exchanges on 1,3,4-Trisubstituted 1,2,3-Triazolium Iodides,” *European J. Org. Chem.*, 2023, doi: 10.1002/ejoc.202300587.

[45] O. Anaya, A. Jourdain, I. Antoniuk, H. Ben Romdhane, D. Montarnal, and E.

Drockenmuller, “Tuning the Viscosity Profiles of High- Tg Poly(1,2,3-triazolium) Covalent Adaptable Networks by the Chemical Structure of the N-Substituents,” *Macromolecules*, vol. 54, no. 7, pp. 3281–3292, 2021, doi: 10.1021/acs.macromol.0c02221.

[46] N. Wolf, L. Kersting, C. Herok, C. Mihm, and J. Seibel, “High-Yielding Water-Soluble Asymmetric Cyanine Dyes for Labeling Applications,” *J. Org. Chem.*, vol. 85, no. 15, pp. 9751–9760, 2020, doi: 10.1021/acs.joc.0c01084.

[47] J. Tang, L. Wan, Y. Zhou, H. Pan, and F. Huang, “Strong and efficient self-healing adhesives based on dynamic quaternization cross-links,” *J. Mater. Chem. A*, vol. 5, no. 40, pp. 21169–21177, 2017, doi: 10.1039/c7ta06650c.

[48] J. V Gulmine, P. R. Janissek, H. M. Heise, and L. Akcelrud, “Polyethylene characterization by FTIR,” *Polym. Test.*, vol. 21, pp. 557–563, 2002.

[49] F. Werlinger and R. S. Rojas, “Evaluation of novel imino-phenol ligands in divalent metal ion extraction / recovery processes from leaching solutions,” *Sep. Purif. Technol.*, vol. 252, p. 117451, 2020, doi: 10.1016/j.seppur.2020.117451.

[50] L. Yang, F. Zhang, T. Endo, and T. Hirotsu, “Microstructure of maleic anhydride grafted polyethylene by high-resolution solution-state NMR and FTIR spectroscopy,” *Macromolecules*, vol. 36, no. 13, pp. 4709–4718, 2003, doi: 10.1021/ma020527r.

[51] J. E. Bara and K. E. O’Harra, “Recent Advances in the Design of Ionenes: Toward Convergence with High-Performance Polymers,” *Macromol. Chem. Phys.*, vol. 220, no. 13, pp. 1–17, 2019, doi: 10.1002/macp.201900078.

[52] Z. Wang *et al.*, “Dynamically Cross-Linked Waterborne Polyurethanes: Transalkylation Exchange of C-N Bonds Toward High Performance and Reprocessable Thermosets,” *ACS Appl. Polym. Mater.*, vol. 4, no. 8, pp. 5920–5926, 2022, doi: 10.1021/acsapm.2c00794.